TRANSIENT HEAT AND MASS TRANSFER IN SOILS*

J. Y. BALADI, D. L. AYERS

Fluid Systems Laboratory, Westinghouse Electric Corporation,
West Lafayette, IN 47906, U.S.A.

and

R. J. SCHOENHALS

Department of Mechanical Engineering, Purdue University,
West Lafayette, IN 47906, U.S.A.

Abstract — Transient heat and mass transfer in soil surrounding a buried heat source are considered. One-dimensional (spherical) models are developed to predict the coupled heat and moisture migration phenomena. Numerical solutions of the exact formulation are given. In addition, two types of closed-form solutions are derived employing approximate models. Experimental measurements are presented for two disparate soil types — a well-graded loam (slow hydraulic response) and sand (more rapid hydraulic response). Predicted and measured temperature variations at the heat source surface are compared. In all cases the numerical solution of the exact formulation agrees with the experimental data reasonably well. The closed-form solutions deviate somewhat from the measurements, but are shown to be useful for obtaining approximate predictions in a simple manner.

NOMENCLATURE

a, heat source radius [m];

c, specific heat [J/kg K];

D_l, hydraulic diffusivity [m^2/s];

D_v, mass diffusivity for air–water vapor [m^2/s];

F_l, specific liquid phase heat of transport [J/kg];

$f(T)$, vapor diffusion function defined by equation (6) [kg/s m K];

g, acceleration of gravity [m/s^2];

h, specific enthalpy, latent heat [J/kg];

J, mass flux [kg/m^2 s];

k, thermal conductivity [W/m K];

k_e, equivalent conductivity, equation (20) [W/m K];

k_l, hydraulic conductivity [m/s];

P, pressure, partial pressure [N/m^2];

p, porosity [m^3/m^3];

q, heat source output [W];

q'', heat flux [W/m^2];

R, gas constant [J kg K];

r, radius [m];

T, absolute temperature [K];

ΔT_u, ultimate steady state temperature rise at heat source surface, aq''_h/k [K];

t, time [s];

u, specific internal energy [J/kg];

v, specific volume [m^3/kg];

x, dimensionless length, $(r - a)/a$;

y, dimensionless temperature, $(1 + x)\zeta$;

z, dimensionless water content, $(1 + x)\xi$.

Greek symbols

α, thermal diffusivity, $k/\rho c$ [m^2/s];

α_e, equivalent thermal diffusivity, $k_e/(\rho c)_e$ [m^2/s];

β, geometrical factor in the vapor diffusion law;

ζ, dimensionless temperature $(T - T_i)/\Delta T_u$;

θ, volumetric moisture content [m^3/m^3];

$\Delta\theta_u$, ultimate steady state decrease in moisture content at heat source, equation (22) [m^3/m^3];

ξ, dimensionless moisture content $(\theta_i - \theta)/\Delta\theta_u$;

λ_e, equivalent Lewis number, α_e/D_l;

ρ, density [kg/m^3];

τ, Fourier number, $\alpha t/a^2$.

Subscripts

a, for air, median value;

c, critical value;

d, dry region;

e, equivalent value;

h, heat source;

i, initial;

l, liquid;

lm, matrical liquid;

lt, thermal liquid;

lv, change from liquid to vapor phase;

m, matrically induced;

pa, air at constant pressure;

pv, water vapor at constant pressure;

s, soil;

t, thermally induced;

v, vapor;

va, air at constant volume;

vv, water vapor at constant volume.

Superscripts

( )$^{+}$,   positive side of interface;

( )$^{-}$,   negative side of interface.

INTRODUCTION

THE TRANSIENT response of wet soils to heating is important in a number of natural processes and engineering applications, including warming of the earth by the sun and heating of soil by underground electrical installations. Examples of the latter are transmission lines and distribution transformers which generate heat due to dissipation of electrical energy. Another recent example involves the use of waste heat from power plants for soil warming to enhance agricultural production. In this application water carrying the rejected power plant energy is typically circulated in pipes buried in the soil.

These engineering applications are represented by a heat source buried underground such as the one shown in Fig. 1. The rejected heat can dry out the surrounding region due to evaporation. Vapor diffuses away from the heat source and condenses in the cooler outer regions. This sets up a liquid concentration gradient which causes some of the moisture to be drawn back by capillary action toward the source. The drying process can increase the thermal resistance of the soil, and this effect can produce higher heat source temperatures than would otherwise occur. These higher temperatures, in turn, drive out more liquid causing even higher soil resistance. If moisture inflow balances the outflow, the thermal resistance of the soil stabilizes. Otherwise, a dry soil region can develop around the heat source. This can result in permanent equipment damage due to overheating in the case of underground electrical installations. Because of the importance of these kinds of applications it is appropriate to study both the transient thermal and transient hydraulic response of soils and their mutual dependence, or coupling.

Much research has been done on heat transfer and mass flows in soils. A few key pertinent investigations will be discussed briefly. Smith [1], Phillip and deVries [2], and Woodside and Kuzmak [3] have postulated a moisture transfer model consisting of a series of evaporation and condensation steps together with a discontinuous flow of liquid film. Nielson *et al.* [4] and Taylor and Cary [5] have applied nonequilibrium thermodynamics to analyze the associated coupling effects. Similar techniques have been employed by Ash and Barrer [6], Mokadam [7], and Vink [8]. Further discussion of pertinent references is contained in [9].

It appears that little work has been performed on coupled heat and mass transfer under transient conditions. Sepaskhah *et al.* [10] and Slegel and Davis [11] report experimental and analytical work on heat and mass transfer in heated and irrigated soils. A report containing information on soil warming applications by means of power plant waste heat has been published by Knudsen and Boersma [12].

It should be noted that the investigations reported in [10] and [11] are somewhat similar to the present study, but they deal with a different geometrical arrangement which is associated with soil irrigation and soil warming applications. In the present work spherical symmetry is employed and liquid sources are not considered, but a more detailed evaluation of the transport phenomena is performed.

This paper describes an investigation of the physics of transient coupled heat and mass transfer in soils, including coordinated analytical and experimental studies. The specific system considered is that of a spherical heat source, buried in an essentially infinite soil of uniform composition, temperature and moisture content, which is subjected to the sudden application of a constant heating rate. The various applicable physical processes are discussed in the analytical formulation. In the present study analysis of the problem led to three different methods of predicting the soil transient response. These methods differ in the degree of sophistication and also, correspondingly, in the amount of computational effort required and in the error incurred. Experiments were conducted using two different soils, Fox loam (9% clay, 40% silt, 51% sand) and Mason sand (0% clay, 1% silt, 99% sand). These soils have quite different hydraulic properties and thereby exhibit considerable contrast in the effects of water movement on thermal response. Comparisons of experimental measurements and the corresponding results of the three computational methods show reasonably good agreement for the most complex analytical technique, and less favorable agreement for the other two. Further details concerning the work reported in this paper are contained in [9].

ANALYTICAL FORMULATION

The general formulation of the buried heat source problem is quite complex, involving evaporation–condensation processes together with gravity action, soil hysteresis, and other secondary phenomena. For purposes of analysis it is appropriate to simplify the problem substantially by eliminating consideration of effects such as gravity, water table, and changes in surface weather conditions. The major aim here is to isolate and study the dominant physics of the problem in order to determine the major effects of mass transfer upon the heat transfer capability of soil adjacent to the heat source. Spherical symmetry is assumed with transient heat and mass transfer in the radial direction only. A polar coordinate system is chosen with its origin located at the center of a spherical heat source. The source is buried in an essentially infinite, initially uniform mass of soil. The relationships describing the dominant physical phenomena are listed below.

1. Fourier's law of heat conduction:

$$q'' = -k \frac{\partial T}{\partial r}. \tag{1}$$

2. Buckingham–Darcy's law for matrically induced liquid mass flux [13]:

$$J_{lm} = -\rho_l D_l \frac{\partial \theta}{\partial r}. \tag{2}$$

3. Thermally induced liquid mass flux [4]:

$$J_{lt} = -\rho_l k_l \frac{F_l}{gT} \frac{\partial T}{\partial r}. \tag{3}$$

Hence, the total liquid mass flux, based on equations (2) and (3), is

$$J_l = -\rho_l \left(D_l \frac{\partial \theta}{\partial r} + k_l \frac{F_l}{gT} \frac{\partial T}{\partial r} \right). \tag{4}$$

4. Vapor mass flux inside the pore spaces of wet soil [14, 15]:

$$J_v = -\beta(p - \theta) f(T) \frac{\partial T}{\partial r}, \tag{5}$$

where

$$f(T) = \rho_v D_v h_{lv} \frac{1}{R_v T^2} \frac{P}{P - P_v},$$

which can be correlated by

$$f(T) = \frac{8.34 \times 10^5}{T^3 (0.024207 e^{5200/T} - 27444)} \tag{6}$$

as shown in [9].

5. Saturated vapor density–temperature relationship:

$$\rho_v = \frac{2.54 \times 10^8}{T} e^{-5200/T}, \tag{7}$$

which is a semi-empirical expression described in [9].

6. Air density–temperature relationship:

$$\rho_a = \frac{1}{R_a} \left[\frac{P}{T} - \rho_v R_v \right], \tag{8}$$

where the total pressure P is taken to be constant and equal to one atmosphere.

When the above relationships are employed in expressions for mass and energy, the moisture conservation equation becomes:

$$\frac{1}{r^2} \frac{\partial}{\partial r} \left[r^2 \rho_l \left(D_l \frac{\partial \theta}{\partial r} + k_l \frac{F_l}{gT} \frac{\partial T}{\partial r} \right) \right]$$
$$+ \frac{1}{r^2} \frac{\partial}{\partial r} \left[r^2 \beta(p - \theta) \cdot f(T) \frac{\partial T}{\partial r} \right]$$
$$= (\rho_l - \rho_v) \frac{\partial \theta}{\partial t} + (p - \theta) \frac{d\rho_v}{dT} \frac{\partial T}{\partial t} \tag{9}$$

and the energy conservation equation becomes

$$\rho_l \left[D_l \frac{\partial \theta}{\partial r} + k_l \frac{F_l}{gT} \frac{\partial T}{\partial r} \right] c_l \frac{\partial T}{\partial r}$$
$$+ \beta(p - \theta) f(T) \frac{\partial T}{\partial r} c_{pv} \frac{\partial T}{\partial r}$$

$$- J_a c_{pa} \frac{\partial T}{\partial r} + \frac{1}{r^2} \frac{\partial}{\partial r} \left(r^2 k \frac{\partial T}{\partial r} \right)$$
$$+ h_{lv} \frac{1}{r^2} \frac{\partial}{\partial r} \left[r^2 \beta(p - \theta) \cdot f(T) \frac{\partial T}{\partial r} \right]$$
$$= \left[\rho_s c_s + \rho_l \theta c_l + (p - \theta) \left(\rho_v c_{vv} + \rho_a c_{va} + u_{lv} \frac{d\rho_v}{dT} \right. \right.$$
$$\left. \left. - R_a T \frac{d\rho_a}{dT} \right) \right] \frac{\partial T}{\partial t} + (R_a T \rho_a - u_{lv} \rho_v) \frac{\partial \theta}{\partial t}. \tag{10}$$

The air flux J_a in equation (10) can be calculated by integration of the mass conservation equation for air. Hence

$$J_a = -\frac{1}{r^2} \frac{\partial}{\partial t} \int_a^r r^2 (p - \theta) \rho_a \, dr. \tag{11}$$

The initial distributions of temperature and moisture content are assumed uniform, and the values of T and θ far from the source remain equal to these initial values. Thus

$$T(r, 0) = T(\infty, t) = T_i = \text{constant}$$
$$\theta(r, 0) = \theta(\infty, t) = \theta_i = \text{constant}.$$

The boundary conditions at the surface of the heat source are

$$\left(\frac{\partial T}{\partial r} \right)_{r=a} = -\frac{q_h''}{h_{lv} \beta(p - \theta) f(T) + k} \tag{12}$$

$$\left(\frac{\partial \theta}{\partial r} \right)_{r=a} = \frac{\rho_l k_l \dfrac{F_l}{gT} + \beta(p - \theta) f(T)}{\rho_l D_l [h_{lv} \beta(p - \theta) f(T) + k]} q_h''. \tag{13}$$

In dry soils the moisture content is equal to or less than the critical value θ_c. At the critical value of θ, liquid film continuity is broken and the liquid does not flow. Also, retained moisture is so tightly held to the surfaces of the soil particles that evaporation and vapor flux are usually neglected. Hence, for this situation $J_l = J_v = 0$. Further, the air flux J_a is also neglected in this case based on order of magnitude considerations. As a result, for dry soils the single governing equation is the heat diffusion equation,

$$\frac{1}{r^2} \frac{\partial}{\partial r} \left(r^2 \frac{\partial T}{\partial r} \right) = \frac{1}{\alpha_d} \frac{\partial T}{\partial t}, \tag{14}$$

where

$$\alpha_d = \frac{k_d}{\rho_s c_s + \rho_l \theta_d c_l}.$$

Again, the presence of air and water vapor is neglected, based on order of magnitude considerations, in the expression for the heat capacity. For this dry soil situation the initial and boundary conditions are written as

$$T(r, 0) = T(\infty, t) = T_i$$

$$\left(\frac{\partial T}{\partial r} \right)_{r=a} = -\frac{q_h''}{k_d}.$$

In the general case of an initially wet soil, a dry–wet interface may be established. This case is shown in Fig. 1. The moisture content throughout the dry region becomes constant and equal to the critical value θ_c, and all mass fluxes are essentially zero in this region. On the other hand, moisture content in the wet region is a function of space and time, and in this region mass flow can be very significant. Equations (9) and (10) on the one hand and equation (14) on the other are the governing equations in the wet and dry regions, respectively. The conditions at the interface separating the two regions are

$$\left(\frac{\partial T}{\partial r}\right)_{r_d^+} = -\frac{\rho_l D_l}{\rho_l k_l \dfrac{F_l}{gT} + \beta(p - \theta_c) f(T)}\left(\frac{\partial \theta}{\partial r}\right)_{r_d^+}$$

(15)

$$\left(\frac{\partial T}{\partial r}\right)_{r_d^-} = \frac{h_{lv}\beta(p - \theta_c) f(T) + k_d}{k_d}\left(\frac{\partial T}{\partial r}\right)_{r_d^-},$$

(16)

where r_d^+ refers to the wet side of the interface and r_d^- refers to the dry side. It should be noted that a dry–wet interface does not occur in every case of an initially wet soil.

In summary, for the case of a dry soil the temperature distribution is obtained from equation (14). For the case of an initially wet soil in which a dry–wet interface does not form, the moisture and temperature distributions are obtained from equations (9) and (10). And finally, for the case of an initially wet soil in which a dry–wet interface does form, the distributions in the wet region are obtained from equations (9) and (10) while the temperature distribution in the dry region is obtained from equation (14). Equations (15) and (16) are used to couple the solutions at the dry–wet interface for this last case.

For the case of initially dry soil, the classical solution of equation (14) with the indicated initial and boun-

FIG. 1. Buried heat source.

dary conditions is given in many texts [16]. This solution is

$$y = \text{erfc}\left(\frac{x}{2\sqrt{\tau}}\right) - e^{x+\tau}\text{erfc}\left(\frac{x}{2\sqrt{\tau}} + \sqrt{\tau}\right).$$ (17)

where $y = (1 + x)\zeta$, $x = (r - a)/a$, $\zeta = (T - T_i)/\Delta T_u$, $\tau = \alpha_d t/a^2$, and $\Delta T_u = aq_h''/k_d$.

For the case of an initially wet soil the simplest prediction technique involves solving the heat conduction equations while neglecting all effects of mass migration as well as phase change of the water. This consists essentially of solving equation (14) with α_d replaced by α, the thermal diffusivity of the initially uniform soil, assumed constant throughout the process. This 'pure heat conduction model' again leads to equation (17) with α_d and k_d replaced by α and k. Obviously this represents a very crude approximation, especially if a dry–wet interface should form in the actual situation. The great advantage of this method lies in its simplicity, but it fails to account for a number of phenomena that may be important. Specifically, of the four transport mechanisms indicated by items 1–4 at the beginning of this section, only the first (Fourier's law) is employed while the other three are neglected.

A somewhat more refined prediction technique involves simplification of equation (10) by eliminating consideration of convective transport of thermal energy due to mass migration, but retaining the latent heat effect due to phase change. The resulting equation is

$$\frac{1}{r^2}\frac{\partial}{\partial r}\left(r^2 k_e \frac{\partial T}{\partial r}\right) = (\rho c)_e \frac{\partial T}{\partial t},$$ (18)

where

$$(\rho c)_e = \rho_s c_s + \rho_l \theta c_l$$ (19)

is the equivalent heat capacity of the wet soil, and

$$k_e = k + h_{lv}\beta(p - \theta) f(T)$$ (20)

is the equivalent conductivity of the soil. If k_e and $(\rho c)_e$ are taken to be constant, this model leads to the same classical solution which characterizes the pure heat conduction model, but an equivalent diffusivity, $k_e/(\rho c)_e$, is employed. The equivalent diffusivity accounts for heat conduction according to Fourier's law and portions of the remaining three transport mechanisms (see items 1–4 at the beginning of this section). The purpose of this procedure is to account for effects of mass migration to the maximum extent possible, while still retaining the simplicity associated with the heat conduction equation. This model is referred to as the 'energy conduction model'.

The most accurate prediction technique involves numerical solution of the equations discussed in this section, equations (9)–(16) and the appropriate initial and boundary conditions. Results obtained in this manner account for all of the phenomena discussed previously, and therefore are more accurate than the predictions obtained from the two approximate models.
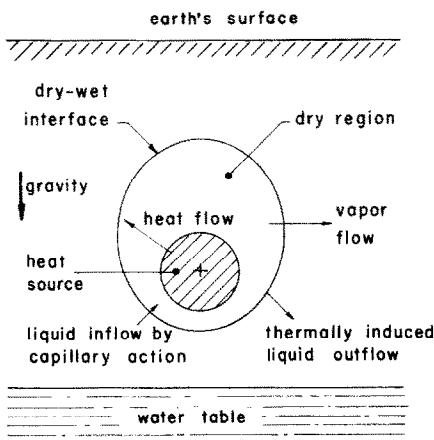
In the Results and Discussion, predictions by all three techniques are compared with experimental measurements. The experimental apparatus and procedure are discussed in the following section.

EXPERIMENTAL PROGRAM

Two types of soils were investigated in this study, a well-graded loam (fine pores and slow hydraulic response) and a plain sand (larger pores and faster response). Their thermal and hydraulic properties were measured using established procedures which are generally accepted in the soil science field.

The measurements of soil dry bulk density ρ_s, porosity p, and specific heat c_s were straightforward. The line source method was used to measure soil thermal conductivity $k(\theta)$. This is an accepted method in soil science which involves measurement or the thermal response of the soil sample as a result of rapid heating by a very small diameter cylindrical heat source. During the brief period of measurement there is not sufficient time for appreciable moisture migration to occur. Hence the k-value determined corresponds to soil in which the moisture is essentially stationary [17]. A pressure plate apparatus was employed to determine soil water suction. The method of Ahuja and Swartzendruber [13] was employed, and an equation for the hydraulic conductivity $k_l(\theta)$ was deduced. Then, one point given by this equation was matched to an experimentally measured value (using a constant head apparatus) to determine both the hydraulic diffusivity

$D_l(\theta)$ and hydraulic conductivity $k_l(\theta)$. The resulting variations of k, k_l, and D_l with moisture content are shown in Figs. 2 and 3 for the two soils tested. Details of these aspects of the experimental work are contained in [9].

Because of difficulties involved in measurements of the geometrical factor β and liquid phase heat of transport F_l, equations (5) and (3), these two properties were not measured. Values within the ranges given in the literature for the two soil types were used instead [4, 15].

A very important aspect of the experimental work was the degree of uniformity of the soil. Consequently, the two soils studied were put through preparation processes to break the aggregates and remove gravel and large organic materials. A power mixer was used to stir the prepared soil with a mist of water in order to bring the moisture content of the soil up to the optimum level. In the vicinity of this optimum value the density of compacted soil becomes insensitive to variations in moisture content. The optimum moisture content was determined by the Standard Proctor Method [18].

The prepared loam was compacted in a tank 1.85 m in height and diameter while the sand was tested in another tank which was 0.92 m in both dimensions. As a result, test runs with loam lasted 200 h while those with sand were terminated after 10 h — before the boundaries of either tank had interfered with the transient processes occurring in the soil during each
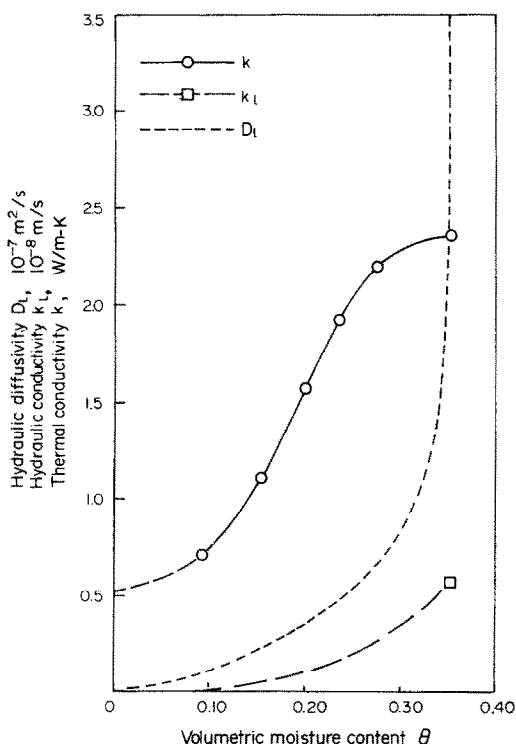
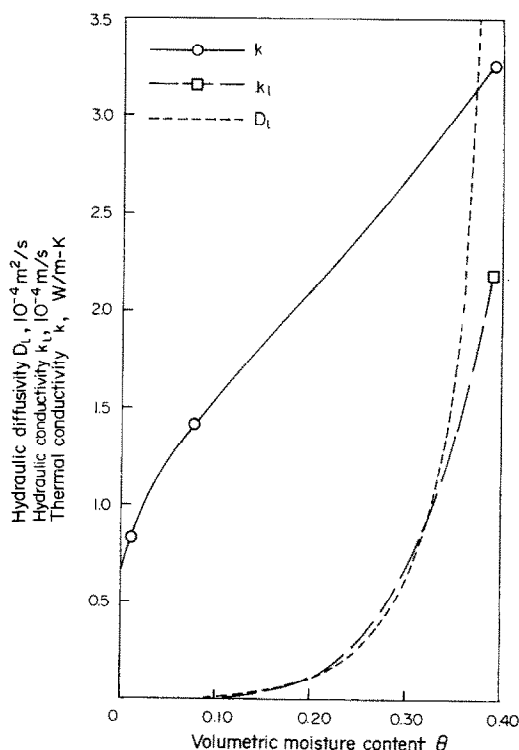FIG. 2. Variations of properties of loam with moisture content.

FIG. 3. Variations of properties of sand with moisture content.

run. That is, during the periods of 200 h and 10 h, respectively, the soils in the two tanks represented infinite media with regard to the transient heat and mass transfer processes.

A heat source 0.02 m in radius was positioned in the center of each tank. This consisted of a copper sphere with an electrical resistance heater imbedded inside. Twenty-nine thermocouples were located vertically along the axis of each tank and horizontally in the central plane of the tank as shown in Fig. 4. This arrangement made it possible to experimentally determine the extent of gravity effects due to free convection and also to check on the initial temperature uniformity of the soil. An electronic scanner and a digital voltmeter were used to sense and record the thermocouple signals.

After preparing the soil volume, several small samples were removed and dried in an oven, with weighing of each sample being performed before and after the drying process. By averaging the results for the various samples a reasonably accurate value was determined for the initial moisture content θ_i. Four moisture probes buried in the soil were used to provide an additional check on the value of θ_i as well as on the uniformity of the initial moisture content. Each probe was composed of two plates separated by an intermediate fiberglass layer. The electrical capacitance of this device is dependent on the moisture content of the fiberglass, which in turn is related to that of the surrounding medium. Transient measurements of the moisture content θ were also obtained with these probes. However, the quality of these data was not very good because the probes were too large and their transient response was too slow. Therefore, transient measurements of moisture content are not reported in this paper.
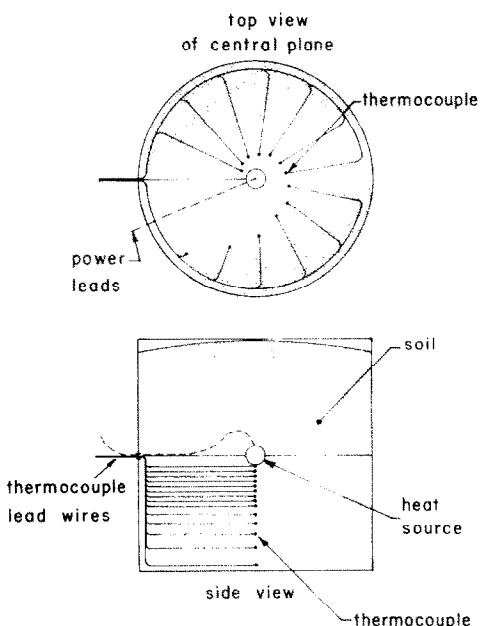

FIG. 4. Experimental apparatus.

Once the uniform soil, heat source and probes were in place, electrical power was supplied to the heat source at a constant rate. A number of transient tests were performed. Conditions and initial values of some of the properties associated with eight representative cases are summarized in Table 1. In connection with the initial property values shown it should be mentioned that the numerical solution accounted for variable properties during the transient period.

RESULTS AND DISCUSSION

Experimental measurements for the eight test runs indicated in Table 1 are shown in Figs. 5–7. Only measurements at the surface of the heat source are shown. In most applications the temperature at the source is of greatest interest. Temperatures at other locations for any given time lie between the initial temperature and the temperature at the source. Measurements obtained at various radii, as indicated in the previous section, were also plotted but are omitted here for the sake of conciseness.

Each experimentally obtained temperature response is compared with the corresponding analytical predictions. Results for loam are given in Fig. 5. For each case the pure heat conduction model predicts a rise in temperature with time. The energy conduction model predicts a similar rise, but for any given time the predicted temperature rise is smaller. This is explained by the fact that the equivalent conductivity k_e characterizing that model is larger than the actual soil thermal conductivity k, since the former represents both heat conduction and energy transport associated with the latent heat due to phase change. Hence, according to this model the moist soil acts like a substance undergoing pure heat conduction, but with a higher k-value. Consequently, the heat diffuses more readily than is predicted by pure heat conduction alone. The numerical solution accounts for all of the transport mechanisms described in the analytical formulation, and therefore exhibits a greater facility for transport than the two simplified models. For this reason the predicted temperature rise for any given time is lower than the values calculated with the two simplified models. Notice that the pure heat conduction model overpredicts the experimentally observed temperature response, and the energy conduction model does also, but with smaller error. The numerical solution, on the other hand, agrees with the measurements reasonably well. The response for Run No. 1 lies well below that for Run No. 2, which vividly illustrates the enhanced energy transport due to moisture. The initial moisture content θ_i was 0.245 for Run No. 1, and was 0.165 for Run No. 2 (see Table 1).

The results for sand shown in Fig. 6 are similar to those for loam, and the comments given above generally apply to sand as well as loam. However, the two simplified models yield almost identical predictions for Run No. 3. In this case the sand was very wet. The conductivity of liquid water in the pores of wet sand is

Table 1. Summary of conditions and initial properties for experimental tests

Run No.	T_i (°C)	θ_i (m³/m³)	q_h (W)	k (W/m K)	k_l (m/s)	D_l (m²/s)
1-loam	22.2	0.245	20	2.01	1.79×10^{-9}	5.08×10^{-8}
2-loam	20.8	0.165	20	1.24	5.21×10^{-10}	2.50×10^{-8}
3-sand	20.4	0.196	20	2.11	1.01×10^{-5}	1.02×10^{-5}
4-sand	20.7	0.196	40	2.11	1.01×10^{-5}	1.02×10^{-5}
5-sand	20.0	0.070	20	1.36	9.98×10^{-8}	3.06×10^{-7}
6-sand	20.1	0.070	40	1.36	9.98×10^{-8}	3.06×10^{-7}
7-sand	20.3	0.024	20	1.00	8.25×10^{-10}	1.02×10^{-8}
8-sand	20.2	0.024	40	1.00	8.25×10^{-10}	1.02×10^{-8}

Soil	ρ_s (kg/m³)	c_s (J/kg K)	P (m³/m³)	θ_c (m³/m³)	F_l (J/kg)	β (none)
loam	1680	795	0.353	0.055	41.9	2
sand	1560	795	0.390	0.050	4.19	1

much higher than that of the air and water vapor occupying the pores of sand with low moisture content, thus yielding a higher overall conductivity k. Also, for very wet sand the liquid nearly fills the pore spaces, leaving only a very small portion of the pore cross-sectional area for vapor diffusion, thus limiting the latent heat effect due to phase change. Hence, the heat conduction effect is dominant in both simplified models for this case, and for this reason they yield almost identical predictions. Both of them overpredict the observed experimental response because they fail to account for transport due to liquid migration, which is a substantial effect for very wet sand. The numerical solution does account for this, as well as all the other effects, and it therefore predicts the experimentally observed response quite well. For Run No. 5 the moisture content is smaller, and the prediction based on the energy conduction model falls somewhat below the prediction based on the pure heat conduction model, as expected. The numerical solution and the

experimental measurements fall together below these two predictions, in a manner similar to the results for loam shown in Fig. 5. In Run No. 7 the initial moisture content θ_i was below the critical moisture content θ_c (see Table 1), so the soil can be regarded as essentially dry throughout the process. Since moisture migration is virtually nonexistent in this case the pure heat conduction model provides a sufficiently accurate prediction. Predictions based on the energy conduction model and the numerical solution are not illustrated, but both of these are identical to the result shown based on the pure heat conduction model. The prediction agrees reasonably well with the measurements for the first hour. But for larger values of time the analysis somewhat overpredicts the observed temperatures.
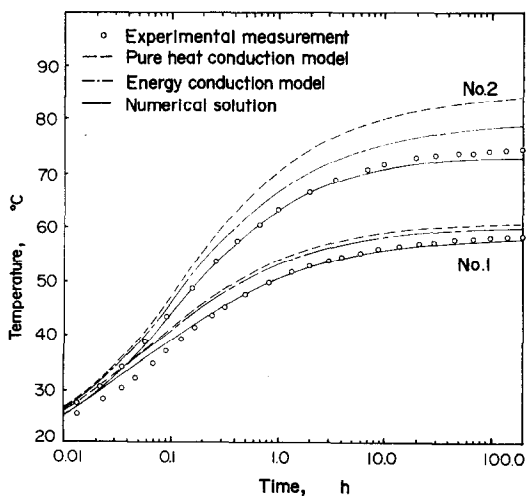
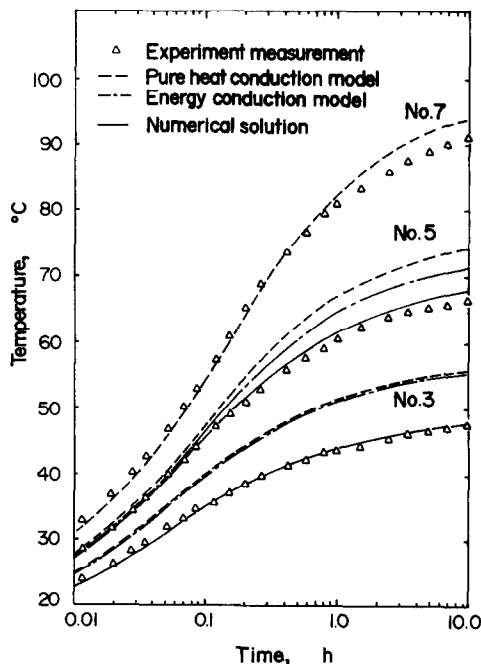FIG. 5. Temperature responses for loam at the surface of the heat source ($q_h = 20$ W).

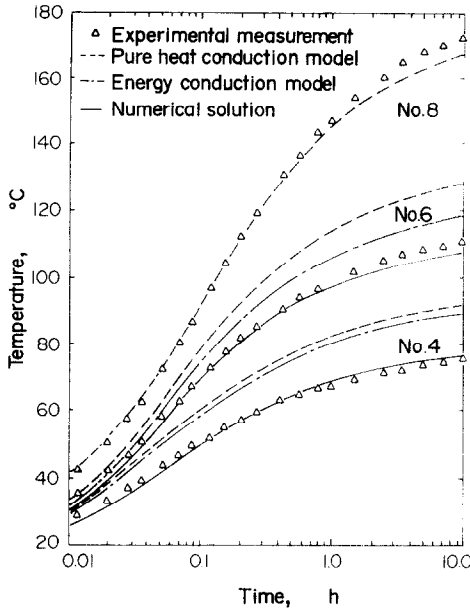FIG. 6. Temperature responses for sand at the surface of the heat source ($q_h = 20$ W).

FIG. 7. Effects of high heat flux for sand $(q_h = 40 \text{ W})$.

Figure 7 shows results similar to those given in Fig. 6, but for a heating rate twice as high. Temperatures rise more rapidly, as expected, with essentially dry sand exhibiting temperatures well above 100°C (Run No. 8).

It should be mentioned that all of the analytical predictions shown in Figs. 5–7 were adjusted to account for the thermal inertia of the heat source. Although the electrical heater element provided a constant heating rate, a fraction of the energy was required to raise the temperature of the source itself, such that the heat transfer rate from the source surface to the soil was not quite constant. This adjustment had the effect of shifting the analytical curves slightly to the right for small values of time. The adjustment was negligible for times in excess of 0.2 h.

It has been previously explained that the numerical solution accounts for convective transport of thermal energy due to mass migration, while the energy conduction model does not. Hence, the deviation of these two predictions is due to this effect. For wet sand (Runs No. 3 and 4) this is a substantial effect. By comparison, wet loam (Runs No. 1 and 2) exhibits some influence of this mechanism, but percentage-wise it is smaller than in the case of wet sand. This difference was traced to the fact that in this range of moisture content the equivalent Lewis number of wet loam is considerably larger than unity, while for sand it is considerably smaller than unity. In the former case equation (9) can be reduced to a diffusion type equation, the solution of which is

$$z = \text{erfc}\left(\frac{x}{2\sqrt{(\tau/\lambda_e)}}\right) - e^{x+\tau/\lambda_e}\text{erfc}\left(\frac{x}{2\sqrt{(\tau/\lambda_e)}}\right.$$
$$\left. + \sqrt{(\tau/\lambda_e)}\right), \qquad (21)$$

where $\lambda_e = \alpha_e/D_l$ is the equivalent Lewis number, based on the equivalent thermal diffusivity, $z = (1 + x)\xi$, $\xi = (\theta_i - \theta)/\Delta\theta_u$, and

$$\Delta\theta_u = \frac{\rho_l k_l \dfrac{F_l}{gT} + \beta(p - \theta)F(T)}{\rho_l D_l} \Delta T_u. \qquad (22)$$

Recall that the 'energy conduction model' leads to equation (17) with α_d and k_d replaced by α and k as discussed earlier. By comparing this equation and equation (21), it can be seen that the change of z with τ is much slower than of y with τ because of the existence of λ_e in equation (21). As a result, at large values of λ_e, moisture migration is very small and, hence, the convective transport of energy is small. For this reason, predictions of the numerical solution and of the 'energy conduction model' are closer together for wet loam. See [9] for further discussion.

It was found that thermocouples in the loam at equal radii, below the heat source and in the central horizontal plane (Fig. 2), indicated essentially the same temperature at any instant of time. This showed that free convection effects within the soil had little effect in distorting the spherical symmetry of the transient temperature distribution. Temperature differences of the order of 1°C or less were observed for loam, and some of this discrepancy may have been due to inaccuracy in thermocouple location. The same behavior was observed for dry sand. For wet sand, however, thermocouples in the central horizontal plane indicated slightly higher temperatures than the thermocouples along the vertical axis at equal radii. The largest difference observed was 4°C, but typically the difference was smaller than this. Thus, it can be said that there was a small but discernible effect of free convection within wet sand.

The numerical solution program contained provision for handling the occurrence of a dry–wet interface, as explained previously. For the eight test runs listed in Table 1, only Run No. 6 exhibited this phenomenon in the numerical solution. It can be seen from Fig. 7 that the source surface temperature exceeded 100°C (boiling point of water), thus indicating the existence of a dry–wet interface. The numerical solution for this case indicated that the dry–wet interface remained essentially at the heat source surface within the 10 h time period of the test run. This prediction is in agreement with the observed thermocouple responses. Only thermocouples attached to the surface of the heat source indicated temperatures in excess of 100°C. Since the remaining thermocouples closest to the heat source were 0.01 m from the surface, these measurements showed that the dry–wet interface did not move more than 0.01 m from the surface during the test. It should be mentioned that Run No. 8 also exhibits temperatures in excess of 100°C, but in this case the sand was initially dry making the formation of a dry–wet interface impossible.

CONCLUSIONS

Based on results obtained in this investigation the following conclusions are drawn:

1. For a given soil energy transport is facilitated by higher moisture content, thus yielding lower temperatures in comparison with the same soil with a lower moisture content.

2. The numerical solution characterizing the complete formulation of the problem predicts the transient thermal response of soils reasonably well.

3. For well-graded moist soils, such as loam, the energy conduction model yields approximate predictions that are adequate for many engineering applications.

4. For porous moist soils, such as wet sand, convective transport of thermal energy due to mass migration is appreciable. For this situation predictions based on the energy conduction model yield considerable error. Use of the numerical solution procedure is recommended for these cases when higher accuracy is desired.

5. For initially dry soils the pure heat conduction model provides accurate predictions. For moist soils this simplified procedure yields approximate predictions only, with errors that are generally greater than those associated with the energy conduction model.

6. Both simplified models overpredict the transient temperature rise.

REFERENCES

1. W. O. Smith, Thermal transfer of moisture in soils, *Trans. Am. Geophys. Un.* **24**, 511–523 (1943).
2. J. R. Philip and D. A. deVries, Moisture movement in porous materials under temperature gradients, *Trans. Am. Geophys. Un.* **38**, 222–232 (1957).
3. W. Woodside and J. M. Kuzmak, Effect of temperature distribution on moisture flow in porous materials, *Trans. Am. Geophys. Un.* **39**, 676–680 (1958).
4. D. R. Nielsen, R. D. Jackson, J. W. Cary and D. D. Evans, *Soil Water.* American Society of Agronomy and Soil Science Society of America, Madison, Wisconsin (1972).
5. S. A. Taylor and J. W. Cary, Analysis of the simultaneous flow of water and heat or electricity with the thermodynamics of irreversible processes, in *7th International Congress of Soil Science Transactions*, Vol. 1, pp. 80–90 (1960).
6. R. Ash and R. M. Barrer, Three phase flow in a temperature gradient, *Trans. Faraday Soc.* **59**, 2260–2267 (1963).
7. R. G. Mokadam, Application of the thermodynamics of irreversible process to the flow of a multicomponent liquid through porous media, *Int. Chem. Engng* **3**, 571–576 (1963).
8. H. Vink, Diffusion in porous media, *Ark. Kemi* **17**, 311–317 (1962).
9. J. Y. Baladi, Transient heat and mass transfer in soils, Ph.D. Thesis, Purdue University, West Lafayette, Indiana (May 1975).
10. A. R. Sepaskhah, L. L. Boersma, L. R. Davis and D. L. Slegel, Experimental analysis of a subsurface soil warming and irrigation system utilizing waste heat, American Society of Mechanical Engineers Paper No. 73-WA/HT-11, Winter Annual Meeting, Detroit, Michigan (November 1973).
11. D. L. Slegel and L. R. Davis, Transient heat and mass transfer in soils in the vicinity of heated porous pipes, *J. Heat Transfer* **99C**(4), 541–546 (1977).
12. J. G. Knudsen and L. L. Boersma, Future developments in waste heat utilization, Summary Report of a National Workshop held at Portland, Oregon, 16–17 December 1964, Circular No. 49. Engineering Experiment Station, Oregon State University (September 1975).
13. L. R. Ahuja and D. Swartzendruber, An improved form of soil water diffusivity function, *Soil Sci. Soc. Am. Proc.* **36**(1), 9–14 (1972).
14. J. W. Cary, An evaporation experiment and its irreversible thermodynamics, *Int. J. Heat Mass Transfer* **7**, 531–538 (1964).
15. J. W. Cary, Water flux in moist soil: thermal versus suction gradients, *Soil Sci.* **100**, 168–175 (1965).
16. H. S. Carslaw and J. C. Jaeger, *Conduction of Heat in Solids*, 2nd edn. Oxford University Press, London (1959).
17. R. D. Jackson and S. A. Taylor, *Methods of Soil Analysis, Part I*, Chapter 26, pp. 349–360. (Edited by C. A. Black), American Society of Agronomy (1965).
18. *ASTM Standards*, Part 4, Philadelphia, PA (1961).

TRANSFERTS VARIABLES DE CHALEUR ET DE MASSE DANS LES SOLS

Résumé—On considère les transferts variables de chaleur et de masse dans le sol entourant une source de chaleur enterrée. On développe des modèles monodimensionnels (sphérique) pour estimer les phénomènes couplés de migration de chaleur et d'humidité. Des solutions numériques de la formulation exacte sont données. Deux types de solutions littérales sont obtenues en utilisant des modèles approchés. Des mesures expérimentales sont présentées pour deux types de sols: une argile bien homogène (réponse hydraulique lente) et un sable (réponse hydraulique plus rapide). On compare les variations de température calculées et mesurées à la surface de la source de chaleur. Dans tous les cas la solution numérique de la formulation exacte s'accorde assez bien avec les résultats expérimentaux. Les solutions littérales s'écartent des mesures mais elles sont utiles pour obtenir de façon simple des estimations approchées.

INSTATIONÄRER WÄRME- UND STOFFTRANSPORT IM ERDBODEN

Zusammenfassung — Der instationäre Wärme- und Stofftransport in der Umgebung einer im Erdboden verlegten Wärmequelle wird betrachtet. Es werden eindimensionale (sphärische) Modelle entwickelt, um die gekoppelten Wärme- und Stofftransportvorgänge zu berechnen. Dazu werden mit Hilfe von Näherungsmodellen zwei Arten von geschlossenen Lösungen hergeleitet. Die Ergebnisse experimenteller Messungen an zwei verschiedenen Bodenarten werden vorgelegt — für einen gut gesiebten Lehm (langsames hydraulisches Ansprechen) und Sand (schnelleres hydraulisches Ansprechen). Die vorausberechneten und die gemessenen Temperaturänderungen an der Oberfläche der Wärmequelle werden miteinander verglichen. In allen Fällen stimmt die numerische Lösung des genannten Ansatzes mit den experimentell ermittelten Daten ziemlich gut überein. Die geschlossenen Lösungen weichen von den Messungen zwar etwas ab, sind aber — wie gezeigt wird — brauchbar, um auf einfache Weise Näherungslösungen zu erhalten.

НЕСТАЦИОНАРНЫЙ ТЕПЛО- И МАССОПЕРЕНОС В ПОЧВЕ

Аннотация — Рассмотрен нестационарный процесс тепло- и массопереноса в почве возле заглубленного источника тепла. Разработаны одномерные (сферические) модели для расчета взаимосвязанных явлений тепло- и влагопереноса. Приведены численные решения задачи в полной постановке. Кроме того, с помощью приближенных моделей получено два типа решений в замкнутом виде. Представлены данные экспериментальных измерений для двух типов почв: хорошо отсортированной глины (медленная гидравлическая реакция) и песка (более быстрая гидравлическая реакция). Проведено сравнение рассчитанных и измеренных значений температур на поверхности источника тепла. Во всех случаях данные численного расчета довольно хорошо согласуются с результатами экспериментов. Решения, полученные в замкнутом виде, дают значения, несколько отличающиеся от измеренных, тем не менее их можно с успехом использовать для простых приближенных расчетов.